Publishing House
AKAPIT

COMPUTER METHODS IN MATERIALS SCIENCE

Informatyka w Technologii Materiałów

Vol. 8, 2008, No. 4

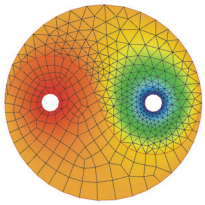

PHASE TRANSITION SIMULATIONS FOR SOLIDIFICATION OF Fe-C ALLOY WITH CELLULAR AUTOMATA INTERFACED WITH SELF-ADAPTIVE HP FINITE ELEMENT METHOD FOR NON-STATIONARY HEAT AND MASS TRANSPORT PROBLEMS

MACIEJ PASZYŃSKI[1*], JERZY GAWĄD[2], PAWEŁ MATUSZYK[2], ŁUKASZ MADEJ[2], DOROTA PODORSKA[3]

[1] Department of Computer Science,
[2] Department of Applied Computer Science and Modelling,
[3] Department of Ferrous Metallurgy,
AGH University of Science and Technology,
Al. Mickiewicza 30, 30-059 Krakow, Poland
[*]Corresponding Author: paszynsk@agh.edu.pl (Maciej Paszyński)

Abstract

The simulation of the phase transition for solidification of Fe-C alloy with the Cellular Automata (CA) method interfaced with the hp-adaptive Finite Element Method (FEM) for the non-stationary heat and mass transport problems is presented in the paper. The computational domain is discretized by the uniform grid for the CA and a sequence of non uniform meshes for the self-adaptive *hp*-FEM. The rule-based CA model is responsible for the simulation of the grow of the new phase within the Fe-C alloy. The self-adaptive hp-FEM generates a sequence of meshes delivering exponential convergence of the numerical error with respect to the mesh size (CPU time). The solution from the previous time step as well as material data from the CA grid are projected to the current self-adaptive hp-FEM. The detailed description of the developed approach as well as the examples of numerical simulations are presented and discussed in the paper.

Key words: *hp*-FEM, Cellular Automata, solidification

1. INTRODUCTION

The numerical simulation of the phase transformation during solidification is a challenging task. This is due to the complex interactions of the phenomena responsible for this process. For example the crystallization of the pure metals and alloys involves the thermal effects connected with the liquid-solid phase transformation as well as with the diffusion and mass transport due to convection. The process depends on the conditions of heat extraction out of the crystallization front. Retaining of the crystallization process continuity is possible if the rate of heat extraction is greater than the heat release rate, which results in the appropriate undercooling of the liquid. The released heat of crystallization increases the temperature in the area close to the crystallization front, while the temperature of the residual liquid remains approximately constant. This process is localized in the very narrow region of crystallization front. This is one of the most significant difficulties for numerical simulations. To capture this very local behaviour an appropriate method has to be applied.

One of the solutions may be the developed hybrid numerical method composed of the discrete CA method and the *hp*-FEM. The self-adaptive *hp*-FEM code was developed by the Demkowicz group

 ISSN 1641-8581

(Demkowicz, 2006; Demkowicz et al., 2007) for the elliptic and Maxwell problems. The code generates a sequence of meshes delivering exponential convergence of the numerical error with respect to the mesh size (number of degrees of freedom d.o.f.), starting with an initial mesh prescribed by the user. The code has been recently extended to support non-stationary problems (Matuszyk & Paszyński, 2007). Therefore, the *hp*-FEM code can be utilized to solve the non-stationary heat and mass transfer problems.

There are many phase transition models considered in the literature, some of them focus on the heat transport problem only (e.g. Zhao & Heinrich, 2001), the mass transport only (e.g. Jacot & Rappaz, 2002), or combined heat and mass transport problems (e.g. Zhu & Stefanescu, 2007; Liu & Liu, 2006). More sophisticated models may also include the fluid flow (e.g. Narski & Picasso, 2007). The interface between the fluid and solid phases can be captured by using the front tracking technique by decoupling solid and fluid phases and introducing some interface conditions (Zhao & Heinrich, 2001; Jacot & Rappaz, 2002; Zhu & Stefanescu, 2007), or by utilizing the Cellular Automata (CA) technique (e.g. Liu & Liu, 2006).

In our model, the material data, such as the thermal conductivity, density and specific heat are calculated on the basis of the CA simulation results. This approach provides the possibility to replicate phase transformation during solidification and to take into account the progressing movement of the crystallization front.

2. CELLULAR AUTOMATA

In the present work the solidification process occurring in the Fe-C system is considered. The carbon is the primary alloying element of steels. Depending on steel grades (low carbon or high carbon), the carbon content can change in the wide range. The case of binary and multi-component alloys requires that analysis of the crystallization includes the variation of composition of solid and liquid phases. If the equilibrium crystallization appears, the diffusion of component in the solid is sufficiently effective to maintain the equilibrium concentration in both phases. In such case the concentration of components is uniform in the whole volume of solid phase. In liquid phase, however, the concentration of alloy component is higher close to the crystallization front, as it is partly rejected by advancing solid, in proportion resulting from the value of equilibrium distribution coefficient (0.19 for C), the cooling rate and the rate of liquid metal flow. Real steel solidification processes proceed in mixed regime, i.e. the concentration of component in solid phase is only partly equilibrated due to back diffusion. The extent of back diffusion depends on the diffusion coefficient of component in solid phase, the translation of solidification front and local solidification time.

The main assumptions of the developed CA code are presented below. The computational domain is discretized using two dimensional rectangular lattice of CA cells. The periodic boundary conditions are imposed at the edges of the lattice. The pseudo-hexagonal neighborhood (Gawąd & Pietrzyk, 2007) is used. This is constructed on the basis of the Moore neighborhood where two randomly selected diagonal cells are removed from the available eight cells. Therefore, the central cell is always surrounded by six neighbors. Similar concept was proposed in (Pezzee & Dunand, 1994), however, in the current work the diagonal cells undergoing removal are independently selected every time the transition rule is activated. This formulation of neighborhood involves probabilistic factor in the simulation. Moreover, the artificial symmetry due to the rectangular lattice is slightly reduced.

The state of the cells in the lattice is updated synchronically in every time step τ. The single increment of the discrete time τ corresponds with continuous time step Δt. The simulation time as well as length of time step are common for both CA and *hp*-FEM simulations. Every CA cell in the lattice is described by the vector of state variables, denoted by $\mathbf{S}_\tau$, comprising of local fraction of solid ($0 \le f_s \le 1$) and increment of solid phase during last time step ($-1 \le \Delta f_s \le 1$). The cell is considered as solid if $f_s = 1$ or liquid if $f_s = 0$, otherwise it represents liquid-solid interface. During every time step the state of each cell in the lattice is updated according to the transition rule, based on the equations described below. The selection of neighborhood N is performed prior to the application of the rule. The pseudo-code approximating the rule of state transition is given in Listing 1.The equilibrium temperature of solidification is given by formula (1) (compare Zhu & Stefanescu, 2007):

$$T_E = T_L\left(c_L^*\right) - \frac{\gamma K}{L} T_m \qquad (1)$$

where $T_L\left(c_L^*\right)$ is equilibrium temperature corresponding with local concentration c_L^* of alloying element, γ is Gibbs energy per inter-phase front area

unit, K is curvature of the interface, L is latent heat of phase transformation, T_m is temperature of solidification at flat surface of interface. The current concentration of alloying element c_L^* is computed by the *hp*-FEM model. The second-order polynomial approximation of the liquidus line $T_L(c)$ is used in the calculations:

$$T_L(c) = 1516.21 - 40.77c - 10.459c^2 \quad (2)$$

```
begin
if (0 < f_s(τ) < 1) ∨ (f_s(τ) = 0 ∧ ∃ k∈ N: f_s(τ)(k) > f_s^c )
then
    Calculate T_E, ΔT, u, Δf_s
    Δf_s(τ+1) ← ϕ(Δf_s,-1,1)
    f_s(τ+1) ← ϕ( f_s(τ) + Δf_s(τ),0,1)
else
    S_τ+1 ← S_τ
    Δf_s(τ+1) ← 0
end
```

Listing 1. *Pseudo-code of CA transition rule*

The velocity of the liquid-solid interface is assumed as a function of local undercooling (Burbelko, 2004):

$$u = C(\Delta T)^n \quad (3)$$

where $\Delta T = T_E - T$, T is local temperature calculated by *hp*-FEM solution of heat transfer equation and C, n are coefficients. In fact, the CA and FEM are coupled with each other by interpolation of the concentration and temperature distribution obtained from *hp*-FEM computations (eq. (2) and (3), respectively).

Increment of solid fraction Δf_s is calculated according to the equation:

$$\Delta f_s = \frac{u\Delta t}{x} \quad (4)$$

where Δt is length of time step and x is linear size of CA cell. The components of state vector $\mathbf{S}_\tau$, are updated using transformation function:

$$\Delta f_{s(\tau+1)} = \phi(\Delta f_s, -1, 1) \quad (5)$$

$$f_{s(\tau+1)} = \phi(f_{s(\tau)} + \Delta f_{s(\tau)}, 0, 1) \quad (6)$$

where ϕ is parametric threshold function, given by the following expression:

$$\phi(x, b_1, b_2) = \begin{cases} b_1 & : \quad x < b_1 \\ x & : \quad b_1 \le x \le b_2 \\ b_2 & : \quad x > b_2 \end{cases} \quad (7)$$

It is also assumed in the model that the cell representing liquid is able to change its state to liquid-solid if it has at least one neighbor of $f_s > f_s^c$. Parameter f_s^c is a critical fraction of solid required for the progress of phase transformation and was assumed as $f_s^c = 0.5$. This parameter indirectly controls the width of the inter-phase zone surrounding the growing crystallite of the solid phase. Actually, the parameter f_s controls the computational thickness of the interface, varying from $f_s^c = 0$ (that corresponds to inifinite diffuse interface) to $f_s^c = 1$ (the thickness of the interface is comparable to the linear size of single CA cell, l). The value of this parameter was selected arbitrary as 0.5, which results in average computational thickness of the interface as approximately $3l$. This selection of f_s improves capability of reproducing the curvature of the interface in CA model without extending of neighborhood radius.

The developed CA model provides values of the fraction of the solid phase and the increase of the fraction of the solid phase, at coordinates of the cells in the CA regular mesh. Since the CA mesh does not coincide with the *hp*-refined meshes generated by the self-adaptive *hp*-FEM, the point-wise material data coming from the CA simulations are approximated by the Smoothed Particle Hydrodynamics (SPH) technique.

3. SMOOTHED PARTICLE HYDRODYNAMICS

The Smoothed Particle Hydrodynamics method with the quintic spline (Vignjevic, 2004) Kernel function in form of:

$$W(R, h_{sm}) = \alpha_d \begin{cases} (3-R)^5 - 6(2-R)^5 + 15(1-R)^5 & 0 \le R < 1 \\ (3-R)^5 - 6(2-R)^5 & 1 \le R < 2 \\ (3-R)^5 & 2 \le R < 3 \\ 0 & R > 3 \end{cases} \quad (8)$$

providing the most accurate approximation results with α_d = 120/ h_{sm}, 7/478π h_{sm}^2, 3/359π h_{sm}^3 has been utilized for smoothing of the discrete CA simulation results. We refer to [13] for more details on the SPH. Based on the continuous SPH approximation of a discrete CA material data, the self-adaptive *hp*-FEM minimizes the numerical error in the H^1 norm.

4. SELF-ADAPTIVE HP FINITE ELEMENT METHOD FOR NON STATIONARY HEAT AND MASS TRANSFER PROBLEMS

The problem of heat and mass transport during the simulation of the phase transition for solidification of Fe-C alloy with moving boundary interface is considered. The simulation from the FEM point of view consists in simultaneous solving the non-stationary heat and mass transfer problems on a sequence of meshes generated by the self-adaptive *hp*-FEM.

The strong form of the non-stationary heat and mass transfer problems is to find $R^2 \supset \Omega \ni x \to T(x) \in R$ temperature distribution field and concentration distribution field $R^2 \supset \Omega \ni x \to c(x) \in R$ satisfying

$$\begin{cases} \rho c_p \dfrac{\partial T}{\partial t} - \nabla \cdot (k \nabla T) = f & on\ \Omega \times I \\ k\mathbf{n} \cdot \nabla T = \beta (T_N - T) & on\ \partial\Omega \times I \\ T(\mathbf{x},0) = T_o & on\ \Omega \end{cases}$$

$$\begin{cases} \dfrac{\partial c}{\partial t} - \nabla (D \nabla c) = 0 & on \quad \Omega \times I \\ \mathbf{n} \nabla c = 0 & on \quad \partial\Omega \times I \\ c(\mathbf{x},0) = c_0 & on \quad \partial\Omega \end{cases} \tag{9}$$

The strong formulations are transformed into the weak variational forms in the following way. Find the temperature distribution $T \in V$ as well as concentration distribution $c \in V$ satisfying

$$\left(\rho c_p \dot{T}, v\right)_\Omega + \int_\Omega k \nabla T \circ \nabla v \, d\Omega + \int_{\Gamma_N} \beta T v \, d\Gamma_N =$$
$$\int_\Omega f v \, d\Omega + \int_{\Gamma_N} \beta u_N v \, d\Gamma_N \quad \forall v \in V$$
$$\left(\rho c_p T(0), v\right)_\Omega = \left(\rho c_p T_0, v\right)_\Omega \quad \forall v \in V \tag{10}$$

and

$$\left(\dot{c}, v\right)_\Omega + \int_\Omega D \nabla c \circ \nabla v \, d\Omega = 0 \quad \forall v \in V$$
$$\left(c(0), v\right)_\Omega = \left(c_0, v\right)_\Omega \quad \forall v \in V \tag{11}$$

where $V = H^1(\Omega)$ and the values of all the parameters: thermal conductivity k, diffusion coefficient D, density ρ and specific heat c_p are obtained from the CA simulations, by using lever-arm principle:

$$X = X_1 f_s + (1 - f_s) X_2 \tag{12}$$

where $X_i \in \{D_i, k_i, c_{pi}, \rho_i\}$, i=1 and i=2 correspond to solid and to the liquid phase, respectively. The thermal effect of phase transformation is taken into account in the right-hand-side term of eq. (9). The power of the heat source in the volume represented by the single CA cell is given by formula:

$$f = \rho L \frac{\Delta f_s}{\Delta t} \tag{13}$$

where: ρ is density, L is latent heat of phase transformation and t is time. Notice, that we do not make use of the front tracking technique (Zhao & Heinrich, 2001; Jacot & Rappaz, 2002; Zhu & Stefanescu, 2007) however, the fraction of the solid phase Δf_s provided by CA is non-zero on the interface only (compare figure 5), and the right-hand-side term of eq. (9) is non-zero on the interface only.

For both the heat and mass transfer problems, the following discretization in time is used:

$$\mathbf{M}\dot{\mathbf{u}} \quad \mathbf{K}\mathbf{u} \quad \mathbf{f} \tag{14}$$

The trapezoidal rule for the time discretization results in the following equation:

$$\mathbf{M} \quad \mathbf{K}\,\mathbf{u}^{k\ 1} \quad \mathbf{M} \quad 1 \quad \mathbf{K}\,\mathbf{u}^{k} \quad \mathbf{f}^{k} \tag{15}$$

where $\mathbf{M}$ is the mass matrix, is the time step, $0,1$ gives different time integration schemes.

5. THE MULTISCALE SIMULATION ALGORITHM

The developed algorithm can be described in the following steps.

(1) The initial temperature $R^2 \supset \Omega \ni x \to T_0(x) \in R$ and concentration $R^2 \quad x \quad c_0 \quad x \quad R$ scalar fields are selected. These fields are presented in figure 1.

(2) The CA simulation is executed. This provides the temperature and concentration fields. As a result, the fraction of the solid phase f_s and the increase of the fraction of the solid phase Δf_s are computed at CA grid nodes.

(3) The SPH smooth approximations of f_s and Δf_s are computed.

(4) The material data and the right-hand-side are computed by utilizing (12) and (13).

(5) The *hp*-FEM is executed to solve the heat and mass transport problems at new time step. Many iterations of the self-adaptive *hp*-FEM code are executed to obtain the solution with

accuracy less than 2% relative error in the energy norm. Actually, there are two instances of *hp*-FEM code executed at this stage, one is used for the heat transport problem and the second one for the mass transport problem, both defined by (9).

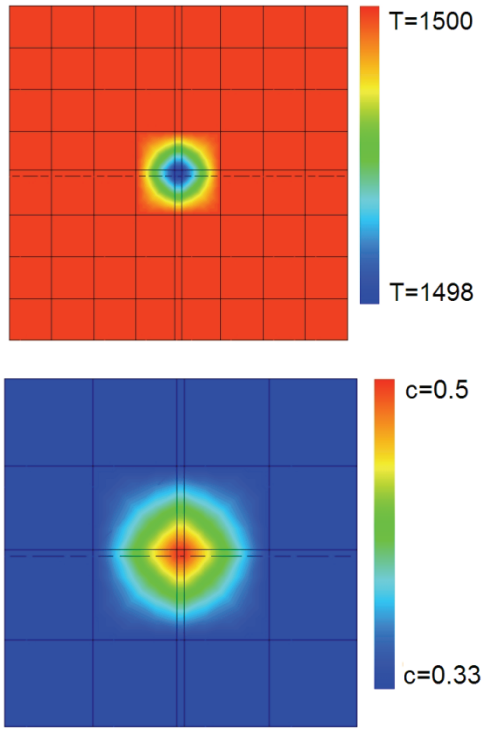

Fig. 1. *The initial temperature and concentration fields (zooms at central parts of the mesh)*

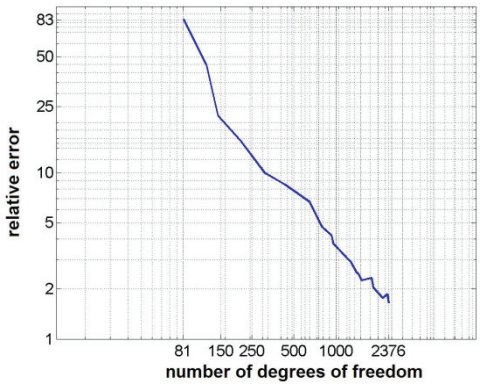

Fig. 2. *The convergence of the self-adaptive hp-FEM for the final time step.*

(6) The two optimal meshes, for the mass and heat transport problem for current time step are backed up to be utilized in the next time step simulations.

(7) The obtained temperature and concentration scalar fields are used in order to compute values at CA grid points.

(8) If the current time step is not the last time step, the time step is updated and the algorithm returns to the step (2).

6. NUMERICAL RESULTS

Examples of the numerical simulation obtained from the developed model for the phase transition in solidification of Fe-C alloy are presented in figures 3-4. The initial temperature and concentration fields are presented in figure 1. The CA simulation was

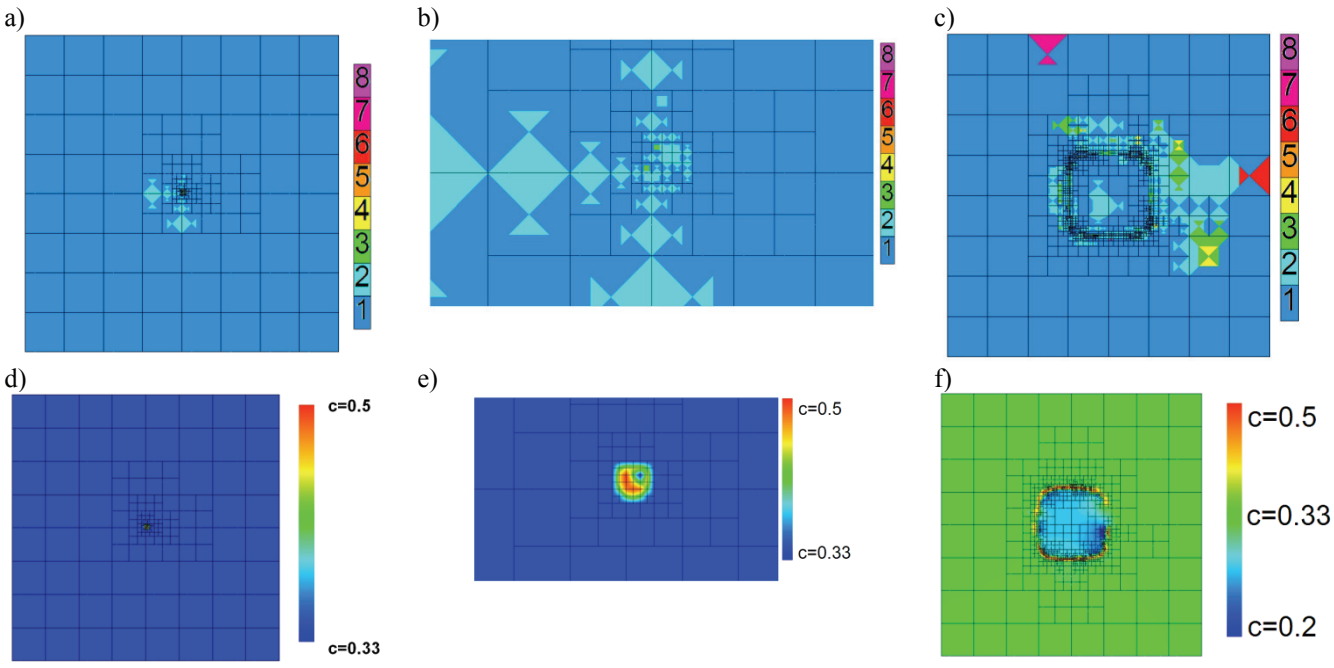

Fig. 3. *The optimal hp-meshes for the concentration field, after several time steps (with zoom at the central part) and the optimal mesh for the final time steps. Colour scale in subfigures a) and c) represents order of polynomial approximation in hp-adapted mesh.*

executed with the presented initial temperature and concentration fields. The material data for the *hp*-FEM, including thermal conductivity k, diffusion coefficient D, density ρ and specific heat c_p were computed with the border values presented in Table 1. The goal of the simulation was to capture grow of the grain during the phase transition phenomenon. Examples of optimal meshes together with computed fields for selected time steps of the simulation are presented in figures 3 and 4. The CA simulation results for the final time step are presented in figure 5. As seen in the figures 3-5 developed model is capable to capture complex material behaviour including also local changes in the crystallization front. This is one of the major advantages of the developed model. The self-adaptive *hp*-FEM for each time step generates a sequence of meshes delivering the exponential convergence of the relative error (in H^1-seminorm) with respect to the number of degrees of freedom, which is illustrated in figure 2

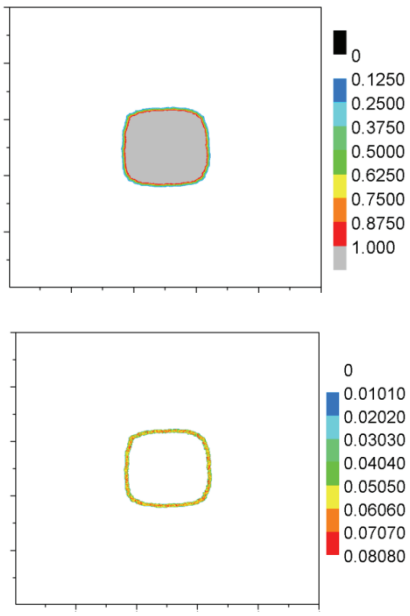

Fig. 5. *The fraction of the solid phase f_s and the increase of the fraction of the solid phase Δf_s for the final time step.*

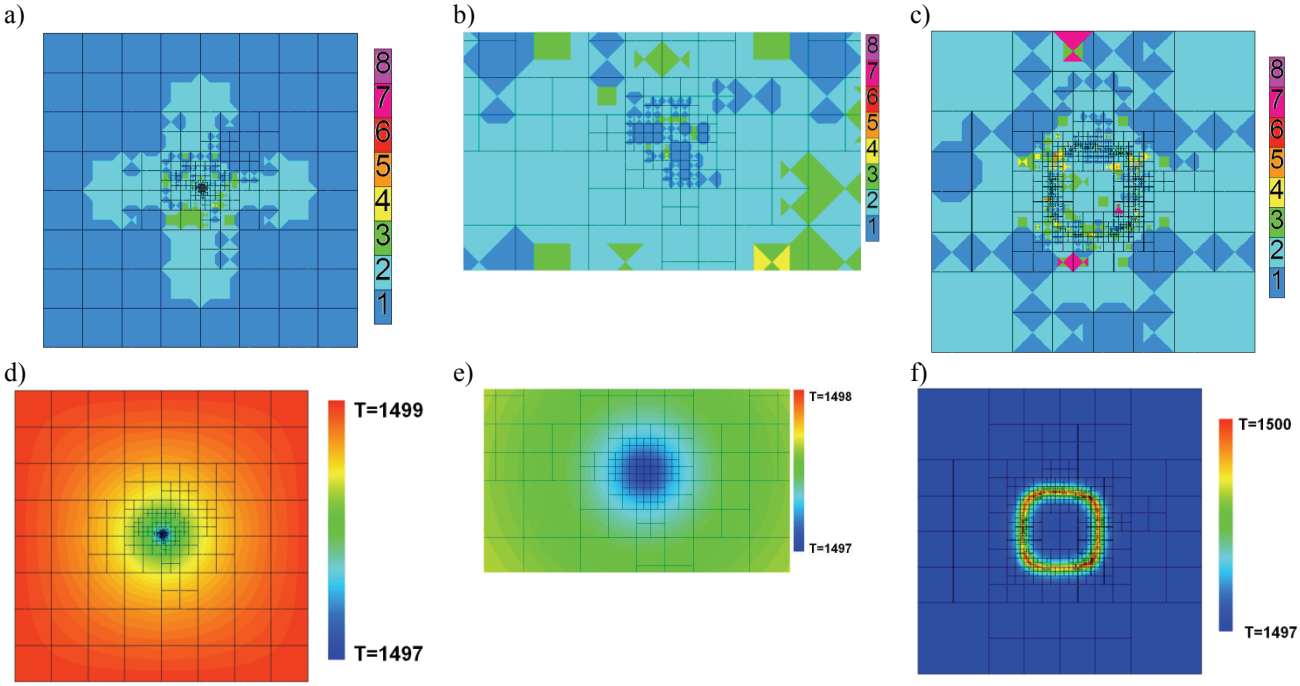

Fig. 4. *The optimal hp-meshes for the temperature field, after several time steps (with zoom at the central part) and the optimal mesh for the final time step. Colour scale in subfigures a) and c) represents order of polynomial approximation in hp-adapted mesh.*

Table 1. *Parameters values for both phases.*

Quantity	Solid phase	Fluid phase	Unit
k	30	15	$W(mK)^{-1}$
D	$1.25 \cdot 10^{-9}$	$5 \cdot 10^{-10}$	$m^2 s^{-1}$
L	$1.97 \cdot 10^{9}$		$J m^{-3}$
ρ	$7.3 \cdot 10^{6}$	$6.8 \cdot 10^{6}$	$g m^{-3}$
c_p	0.450		$J g^{-1} K^{-1}$

for the final time step. The code provided the solution with accuracy 1% relative error in the energy norm, with 2375 degrees of freedom only.

7. CONCLUSIONS

The multi-scale model for the phase transition for solidification of Fe-C alloy, based on the CA model coupled with the self-adaptive *hp*-FEM was presented in this paper. The *hp*-FEM was utilized to

solve the non-stationary heat and mass transfer problems, while the CA model was used in order to compute the fraction of the solid phase and the increase of the fraction.The CA model provided the data allowing calculation of material parameters and heat source within the inter-phase zone for the *hp*-FEM. Meanwhile, the results of *hp*-FEM provided temperature and concentration fields for the CA simulation. The SPH method was utilized to smooth the CA simulation results. The self-adaptive *hp*-FEM generated a sequence of meshes delivering exponential convergence of the solution for every time step of the simulation. One may conclude that the proposed multi-scale algorithm appears useful in solving a wide class of phase transition phenomena.

It's worth to remark that the presented results address an idealized case of solidification process. In real process the carbon that excess over the solubility in solid solution precipitates in the form of carbides. This phase is being formed during steel casting and it has essential influence on grain coarsening, acting as growth inhibitor. Particularly, a presence of elements of high affinity towards carbon, for example Ti, results in formation of carbides at initial stage of casting, even at low cooling rate. If the analysis of process is restricted to a single alloying element only, therefore the effect of compounds precipitation is not taken into account. The precipitation and its influence on crystallite growth will be a subject of further research.

ACKNOWLEDGEMENTS

The support of Polish MNiSW grant no 3 T08B 055 29 is gratefully acknowledged.

REFERENCES

Demkowicz, L., 2006, Computing with hp-Adaptive FE, Vol. I. One and Two Dimensional Elliptic and Maxwell Problems, Chapmann & Hall.

Demkowicz, L., Kurtz, J., Pardo, D., Paszyński, M., Rachowicz, W., Zdunek, A., 2007, Computing with hp-Adaptive FE. Vol. II Frontiers: Three Dimensional Elliptic and Maxwell Problems with Applications, Chapmann & Hall.

Matuszyk, P., Paszyński, M., 2007, Fully automatic 2D hp-adaptive Finite Element Method for Non-stationary Heat Transfer Problems, COMPLAS, Barcelona.

Zhao, P., Heinrich, J. C., 2001, Front-tracking finite element method for dendritic solidification, Journal of Computational Physics, 173, 765-796.

Jacot, A., Rappaz, M., 2002, A pseudo-front tracking technique for the modelling of solidification microstructures in multi-component alloys, Acta Materialia, 50, 8, 1909-1926.

Zhu, M. F., Stefanescu, D. M., 2007, Virtual front tracking model for the quantitative modeling of dendritic growth in solidification of alloys, Acta Materialia, 55, 5, 1741-1755.

Liu, Y., Xu, Q., Liu, B., 2006, A Modified Cellular Automaton Method for the Modeling of the Dendritic Morphology of Binary Alloys, Tsinghua Science & Technology, 11, 5, 495-500.

Narski, J., Picasso, M., 2007, Adaptive finite elements with high aspect ratio for dendritic growth of a binary alloy including fluid flow induced by shrinkage, Computer Methods in Applied Mechanics and Engineering, 196, 37-40.

Gawąd, J., Pietrzyk, M., 2007, Application of CAFE multiscale model to description of microstructure development during dynamic recrystallization, Arch. Metall. Mater., 52, 257-266.

Pezzee, C. E., Dunand, D. C., 1994, The impingement effect of an inert, immobile second phase on the recrystallization of a matrix, Acta Metall., 42, 1509-1524.

Burbelko, A., 2004, Mezomodelowanie krystalizacji metodą automatu komórkowego, Wydawnictwa AGH, Kraków (in polish).

Vignjevic, R., 2004, Review of development of the smooth particle hydrodynamics (SPH) method, Proc. Conf. DCSSS, Cranfield.

SYMULACJA PRZEMIANY FAZOWEJ PRZY KRZEPNIĘCIU STOPU FE-C METODĄ AUTOMATÓW KOMÓRKOWYCH POŁĄCZONYCH Z SAMO-ADAPTACYJNYM HP ROZWIĄZANIEM MES DLA NIESTACJONARNEGO TRANSPORTU CIEPŁA I MASY

Streszczenie

W pracy podjęto próbę symulacji przemiany fazowej za pomocą połączenia metody Automatów Komórkowych (Cellular Automata CA) z rozwiązaniem Metodą Elementów Skończonych (MES) problemu transportu ciepła i masy. Wykorzystane podejście bazuje na dyskretyzacji wspólnej domeny obliczeniowej za pomocą stałej siatki CA oraz hp-adaptowanej siatki MES. Za pomocą modelu CA odtworzono rozrost ziarna nowej fazy, wykorzystując regułowy opis postępu przemiany. Ponieważ na granicy międzyfazowej zachodzi skokowa zmiana własności materiału, a jednocześnie zmienne pole temperatur i koncentracji składników wpływa na lokalną kinetykę przemiany, w obszarze tym przeprowadzono adaptację siatki MES. Natomiast w obszarach odległych od frontu przemiany prowadzone jest rozwiązanie na elementach dużo większych od rozmiaru komórek CA. Pomiędzy MES i CA wprowadzono algorytm wygładzający, oparty na metodzie SPH (Smoothed Particle Hydrodynamics). W pracy zaprezentowany został opis opracowanego modelu wieloskalowego oraz przedstawiono wyniki symulacji przemiany fazowej.

Received: August 3, 2008
Received in a revised form: January 17, 2009
Accepted: January 21, 2009